Journal of Radioanalytical and Nuclear Chemistry, Vol. 265, No. 2 (2005) 303–308

Flux weighted efficiency calibration of The University of Texas at Austin PGAA Facility

S. R. Biegalski,[1]* T. C. Green,[1] G. A. Sayre,[2] W. C. Charlton,[2] D. J. Dorsey,[1] S. Landsberger[1]

[1] *Nuclear Engineering Teaching Laboratory, The University of Texas at Austin, R9000, Austin, TX 78759, USA*
[2] *Department of Nuclear Engineering, Texas A&M University, College Station, TX 77843-3133, USA*

(Received October 12, 2004)

Work was conducted on The University of Texas at Austin Prompt Gamma Activation Analysis Facility located on Beam Port 3 of the 1.1 MW Triga reactor at the Nuclear Engineering Teaching Laboratory. This effort required that the flux weighted detector efficiency be determined. Measurements of the neutron beam intensity as a function of spatial position over the target were conducted. In addition, the point-wise detector efficiency was mapped over the area where the neutron beam hits the sample. The flux-weighted efficiency was then calculated to match the sample geometry. This average efficiency was then utilized for quantitative analysis of the prompt gamma-ray spectra.

Introduction

Quantitative prompt gamma activation analysis (PGAA) requires the calibration of the Ge detectors and associated electronics used for high-resolution gamma-ray spectroscopy. This generally includes the following calibrations: energy versus channel, energy versus detector resolution, and detector efficiency. The energy versus channel and energy versus detector resolution calibrations are normally straight forward. Peaks are found within a spectrum, identified and then fit to a calibration equation. The efficiency of the system may be calibrated through a comparator technique, by a parameterization technique, or by a mix of both.[1] The comparator technique is when a sample of known composition, the comparator, is activated and counted under the same conditions as the sample. The sample composition is then determined by comparing the detector response it produces to the detector response generated by the comparator. The benefit of this method is that the self-absorption, cascade summing, detector efficiency, and the yield of the radionuclide are directly accounted for. While the comparator method sounds ideal, it is often difficult and costly to implement in PGAA for all elements in all sample-to-detector relationships.

A second technique for calibration of PGAA systems is the parameterization method. In this method, one needs to individually determine all the parameters of the measurement process: the efficiency calibrations of the gamma-ray detector, cascade summing effects, self-absorption effects, neutron flux at the sample, neutron cross-sections, and the yields of the radionuclides of interest. The benefit of this method is that one does not need to calibrate with the specific elements one intends to measure. The negative aspect to this method is that the calibration nominally has a higher uncertainty than the comparator method and it is subject to more systematic errors.

The k_0 calibration method is an example of mixing the comparator method with the parameterization method.[2–4] In the k_0 method, a single comparator is used to benchmark a system and counting geometry. Parameterization factors are then used to calculate calibrations for elements other than the one used in the comparator.

This paper focuses on efforts at The University of Texas at Austin to develop a strict parameterization approach to the efficiency calibration of a PGAA facility. This is complicated by the fact that the neutron flux is spatially non-uniform as it emerges from the cold neutron beam guide tubes.[5] Values for gamma-ray yields and neutron cross-sections were taken from values found in the literature. However, point efficiencies for the detector and the flux profile had to be determined experimentally.

Experimental

Experimental setup

Beam port #3 (BP#3) at The University of Texas at Austin (UT) Nuclear Engineering Teaching Laboratory (NETL) contains the Texas cold neutron source (TCNS). Figure 1 shows the TCNS as it was completed in 1995.[6] A detailed description of this facility in its current state may be found in the dissertation of DORSEY (2003).[7] Neutrons from the Triga reactor enter a cold neutron moderating chamber that contains mesitylene (1,3,5-tri-methyl-benzene, C_9H_{12}) frozen to approximately 27 K. The neutrons reach thermal equilibrium with the frozen mesitylene as they travel through this moderator. The moderating chamber may also be purged with helium if moderation to sub-thermal temperatures is not desired.

* E-mail: biegalski@mail.utexas.edu

0236–5731/USD 20.00

Akadémiai Kiadó, Budapest
Springer, Dordrecht

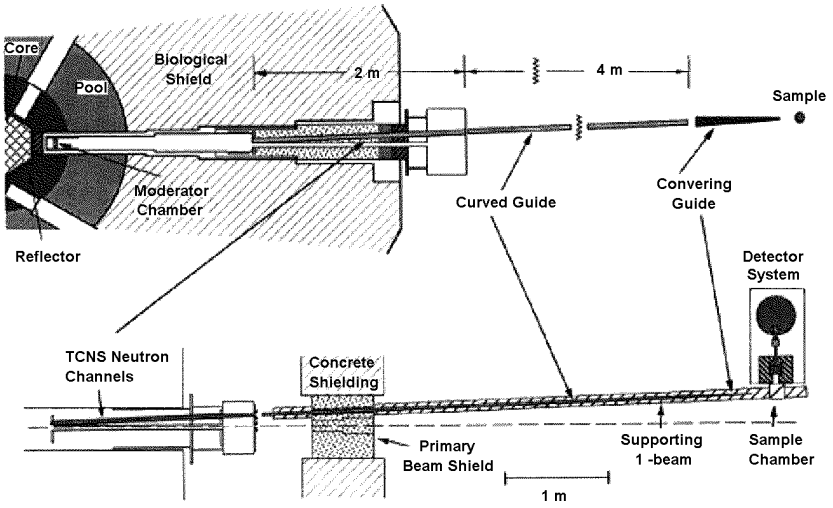

Fig. 1. The Texas cold neutron source (TCNS) as inserted into BP#3 (units are in m)

Figure 1 shows that the moderation chamber is close to the reactor core. The neutrons depart from the moderation chamber and then travel down BP#3 through the reactor biological shielding. Halfway through the shielding, the neutrons enter the curved guide tubes. These neutron guide tubes are curved to a 300 m radius. The neutron guide tubes channel neutrons away from the beam centerline and point them at the sample. Fast neutrons and gamma-rays maintain a straight path down the beam port, so only sub-thermal neutrons interact with the sample. The final guide section is a converging guide that provides a maximum gain of 5.5 at the focal plane 24-cm from the mouth of the guide.[8,9]

The TCNS has thermal equivalent neutron flux of approximately $1.5 \cdot 10^7$ n·cm^{-2}·s^{-1} at the end of the converging guide when the cold neutron source is not operating. With the mesitylene moderator frozen to 27 K, the thermal equivalent neutron flux increases to approximately $4.6 \cdot 10^7$ n·cm^{-2}·s^{-1}.[10] Several sample geometries and holding devices are available for use on the facility. A fluoro-ethylene propylene bag designed to fit over the sample stand may be filled with helium to remove hydrogen, oxygen, and nitrogen background from normal room air.

A horizontal, n-type Ortec GMX Series Gamma-X HPGe coaxial detector system detects the prompt γ-rays generated in the TCNS's sample chamber. This detector has a relative efficiency of 23% and a 0.5 mm thick beryllium window facing the sample. The detector is housed in a lead shield. The shield is six inches thick on all sides with the exception of a two inch collimation hole between the detector and sample. The detector's shielding is on a track that allows experimenters to adjust the detector-to-sample distance.

The TCNS is equipped with a Canberra DSA 2000 digital spectroscopy system. This provides the high voltage power supply, amplifier, and multi-channel analyzer. The MCA is set to 16k channels and the amplifier gain is set so that the spectral span is 12 MeV. The Canberra GENIE 2000 software package is used to control the DSA 2000 unit, collection of the spectra, and for spectral analysis.

Measurement of the neutron flux profile

The spatial distribution of the neutron beam was determined by use of a TH 49424 HX CCD camera from Thompson Tubes Electroniques.[11] The beam was imaged by placing the neutron camera in-line with the neutron beam. The beam was imaged at a power level of 100-kW to prevent the camera from saturating which occurs at higher power levels. It is assumed that the spatial distribution remains consistent at the end of the neutron guide tube for all high reactor power levels at this facility. The linear relationship between reactor power and the beam intensity has been verified by a flux monitor.[12]

Images were taken both with an unperturbed beam as well as with a cadmium disk located at a known point on the sample holder. The cadmium disk position and diameter are then used to scale the neutron beam image and map it to the positions on the sample holder. Thirty 1/30 second 8-bit images were taken of the beam intensity. Each image was converted to a numerical array and then summed in MatLab.

Measurement of detector efficiency

A map of the efficiency of the detector system for a point source located at numerous *(x,y)* positions was created. The point source used was a ^{152}Eu calibration standard from the National Institute for Standards and Technology (NIST). Point source efficiencies were acquired for 48 positions along an equally spaced three

mm cartesian grid across the sample location. Each position was counted for one hour. The target-to-sample distances were large enough that cascade summing was not a significant problem. The efficiency map and radiograph were aligned using the cadmium disk exposure from above.

Results and discussion

Neutron flux profile

Figure 2 shows the neutron flux profile for the TCNS facility. The units for the *x*- and *y*-axis are in pixels. The magnitude of the beam intensity is normalized to unity since only flux shape is needed in these calculations. The beam is roughly rectangular in shape with slightly curved corners and is tightly collimated. Figure 2 shows the definitive structure of the beam. There are two large longitudinal (in the *y*-dimensions) intense oval shapes and one weaker longitudinal oval shape in the beam structure. These are from the guide tube structure.

The absolute *x*- and *y*-dimensions of the beam were determined by aligning the neutron radiograph using a cadmium disk. This allowed for positioning of the neutron beam onto the foil samples and sample holders. The beam is approximately 4.45-cm high (in the *y*-direction) and 1.59-cm wide (in the *x*-direction).

Detector efficiency

Figure 3 shows a map of the detector efficiency over the range of the beam area. The detector is perpendicular to the neutron beam. The sample sits at 45 degrees with respect to both the neutron beam and the detector. The slope of the efficiency map shown in Fig. 3 is a result of different distances to the detector from different parts of the sample.

Flux weighted efficiency calculation

The flux weighted efficiency was then calculated by:

$$\varepsilon_{effective} = \frac{\sum_{i=1}^{n}\sum_{j=1}^{m}\phi_{ij}\varepsilon_{ij}}{\sum_{i=1}^{n}\sum_{j=1}^{m}\phi_{ij}} \quad (1)$$

where $\varepsilon_{effective}$ is the flux weighted efficiency; ϕ_{ij} is the neutron flux at grid position (i, j), and ε_{ij} is the detector efficiency at grid position (i, j).

If the beam is completely encompassed by the sample, the calculation is to be performed for all points in the beam. If the sample lies within the beam, then the weighted flux is to be calculated for only the area that the sample covers. The normalized flux weighted efficiency for the TCNS is shown in Fig. 4.

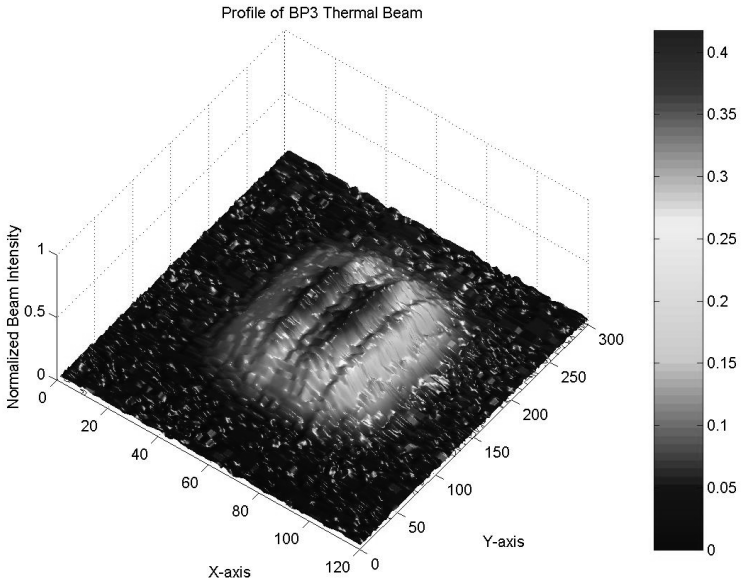

Fig. 2. Neutron beam intensity. The *x*-axis represents the horizontal aspect of the beam

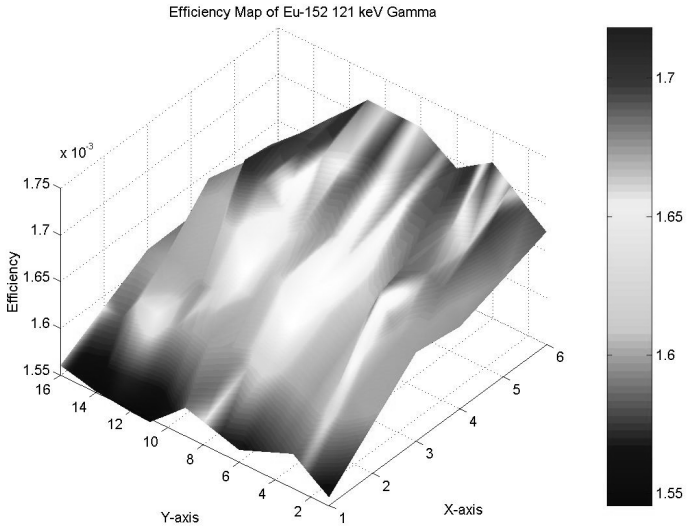

Fig. 3. Efficiency map over beam area. The *x*-axis represents the horizontal aspect of the beam. Each unit the *x*-axis and *y*-axis represents 3 mm at the sample position

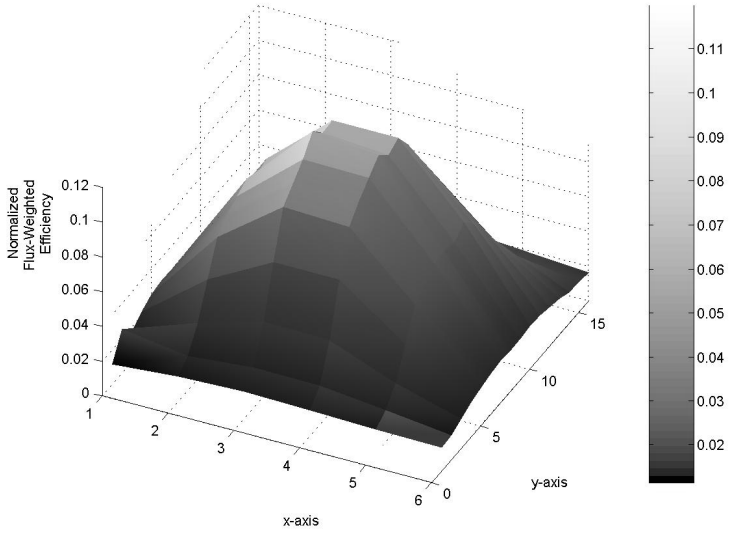

Fig. 4. Normalized flux weighted efficiency of TCNS facility with an average distance of 24 cm between the sample and the detector face. The *x*-axis represents the horizontal aspect of the beam. Each unit the *x*-axis and *y*-axis represents 3 mm at the sample position

Beam magnitude calculations

The magnitude of the beam intensity was quantified by counting a vanadium foil and measuring the activity of the activation product. The gamma-ray acquisition was initiated after an activation time of roughly seven half-lives when saturation activity was reached. ^{52}V ($T_{1/2}$ = 3.743 m) was produced via the (n,γ) reaction with ^{51}V (99.750% naturally abundant). For this work, a 10 cm×10 cm foil sample from Goodfellow was utilized and the neutron beam fit completely in the foil sample. The thermal equivalent flux magnitude was then calculated as:

$$\phi = \frac{\lambda_{52_V} N_{52_V}}{N_{51_V} \sigma_{51_V}} = \frac{Counts}{\varepsilon \ \gamma \ N_{51_V} \sigma_{51_V}} \qquad (2)$$

where ϕ is the neutron flux; N is the number of atoms; σ is the thermal (2200 m·s^{-1}) cross section; λ is the decay constant; *Counts* is the number of counts under the peak

at 1434 keV; ε is the detector peak efficiency at 1434 keV; γ is the ^{52}V gamma-ray yield for the 1434 keV line.

Once the thermal equivalent flux is obtained, it is correlated to the number of neutron counts recorded on a ^{3}He detector measuring the leakage current in the beam. It has been shown that this leakage current is directly proportional to the neutron flux in the beam. Thus, the leakage current measurement may be utilized to monitor the flux impeding on the sample.

For the results in this work, a 99.8% pure V foil from Goodfellow was utilized. The gamma-ray spectrum was initiated 49 minutes after the beam line was opened. This period of time is sufficient for the ^{52}V to reach saturation activity. The spectrum was then collected for 20064.67 seconds (5.6 hours). The number neutrons incident on the sample was calculated to be $4.14 \cdot 10^{11} \pm 4.96 \cdot 10^{9}$ neutrons. The ^{3}He detector measured 10625815 counts during this period. The conversion factor for the ^{3}He detector is then calculated to be $3.89 \cdot 10^{4} \pm 4.67 \cdot 10^{2}$ neutrons per ^{3}He count.

Efficiency curve calculation

An efficiency curve was then calculated using the flux-weighted ^{152}Eu as a base. A prompt gamma-ray spectrum from a V foil measurement was then utilized to extend the efficiency curve out to 7310 keV with a method similar to what is used in MOLNÁR et al. in 2002.[13] DORSEY et al. (2002)[14] applied a similar method at this facility for measurement of water content in carbon composites. The partial gamma-ray cross sections, which are proportional to the gamma-ray intensity or yield, were taken from a new PGAA library underdevelopment by the International Atomic Energy Agency (IAEA).[15] The calculated efficiency values were then fit using a least-squares fitting routine[16] to produce the following average efficiency curve:

$$\begin{aligned}\ln(\varepsilon) = {} & (0.03100987982)\ln(E)^4 - \\ & -(0.8459255035)\ln(E)^3 + \\ & +(8.60770575)\ln(E)^2 - \\ & -(37.84311649)\ln(E) + (66.80949110)\end{aligned} \tag{3}$$

Figure 5 shows a plot of the measured efficiency values and the best-fit curve. The relative uncertainty in the efficiency best-fit curve is estimated to be ±2.9% based on propagations of errors from the peak areas, γ-ray yields, and the χ^2 value for the fit through the averaging procedure for the foil area. These uncertainties were produced by the LSMOD code.[16]

For completeness, the best-fit curve for this data was also compared to the efficiencies produced using the REEDY and FRANKLE library.[17] Good agreement is found between both libraries, however, a systematic bias of approximately 8.15% exists between efficiencies calculated using the two libraries for peaks above 1400 keV. This bias results in the efficiencies calculated using the REEDY and FRANKLE data to be on average 8.15% lower than those calculated using the IAEA library.

Efficiency validation

The efficiency curve was then tested by analyzing a 99.0% pure aluminum standard foil from Goodfellow. The foil was large enough so that the entire neutron beam interacted with the foil. The number of neutrons interacting with the respective samples was monitored with a calibrated ^{3}He detector that measures leakage current on the beam. The number of photons measured in the respective photo-peaks was compared to the theoretically calculated values. Neutron cross section values were taken from the ENDF/B-VI.0 library. Good agreement was found between the calculated yield value for the major Al prompt photons and the values found in both the IAEA and REEDY and FRANKLE libraries. Table 1 shows these values for the major Al prompt gamma-rays.

Table 1. Experimental prompt gamma-ray yields for aluminum

Experimental values		IAEA database[13]		REEDY and FRANKLE database[15]	
Energy, keV	Yield, %	Energy, keV	Yield, %	Energy, keV	Yield, %
3034.0	8.6 ± 0.91	3033.896	7.749	3033.9	8.8
3465.0	7.4 ± 0.80	3465.058	6.320	3465.1	7
4132.7	7.2 ± 0.79	4133.407	6.450	4133.4	6.9
4259.4	7.5 ± 0.82	4259.534	6.623	4259.5	6.8
7723.2	25.2 ± 2.7	7724.027	21.342	7724	26.81

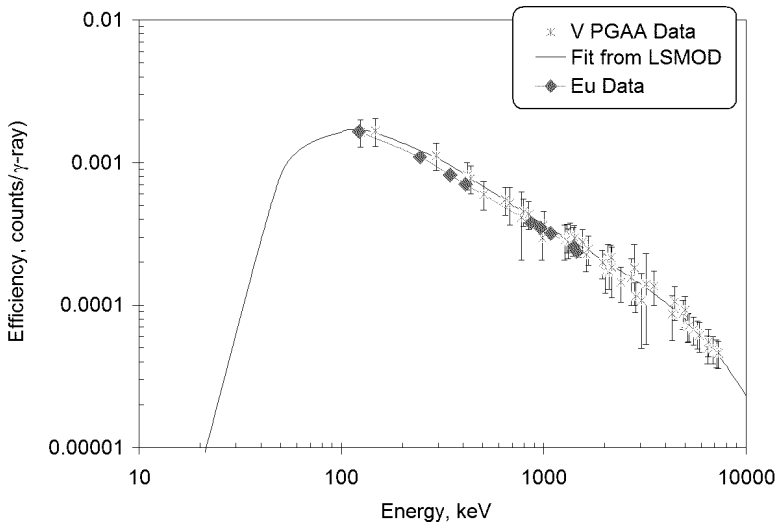

Fig. 5. Detector peak efficiency versus energy for the foil sample (averaged using a flux weighting) with an average distance of 24 cm between the sample and the detector face

Conclusions

This method shows promise for a wide range of applications at the TCNS. It is best suited for irregular geometry samples and for the analysis of elements that are not readily available in standard reference solutions. The negative aspects of this method are that the uncertainty of the efficiency is higher than what is potentially achievable with a comparator method, and the method is highly dependent on the accuracy of published prompt gamma-ray yield data. The benefit of this method is that it provides a parameterization technique for calibrating the PGAA facility for numerous sample geometries.

*

The authors would like to thank the staff at the Nuclear Engineering Teaching Laboratory at The University of Texas at Austin for support and reactor time for this work. The authors would also like to thank Sandia National Laboratory for sponsoring part of this work.

References

1. K. HEYDORN, Neutron Activation Analysis for Clinical Trace Element Research, CRC Press, Boca Raton, Florida, 1984.
2. Z. RÉVAY, G. L. MOLNÁR, Radiochim. Acta, 91 (2003) 361.
3. G. L. MOLNÁR, Z. RÉVAY, R. L. PAUL, R. M. LINDSTROM, J. Radioanal. Nucl. Chem., 234 (1998) 21.
4. F. DE CORTE, Czechosl. J. Phys., 53 (2003) A161.
5. B. W. WEHRING, K. UNLU, C. RIOS-MARTINEZ, Appl. Radiation Isotopes, 48 (1997) 1343.
6. K. UNLU, C. RIOS-MARTINEZ, B. W. WEHRING, Nucl. Instr. Meth., A353 (1994) 397.
7. D. J. DORSEY, Development of Neutron Beam Analytical Techniques for Characterization of Carbon Fiber Composite Materials, Ph.D. Dissertation, The University of Texas at Austin, 2003.
8. J. KIM, Neutron Focusing System for the Texas Cold Neutron Source, Ph.D. Dissertation, The University of Texas at Austin, 1993.
9. J. Y. KIM, B. W. WEHRING, K. UNLU, Trans. Am. Nucl. Soc., 69 (1993) 166.
10. C. RIOS-MARTINEZ, Prompt Gamma Activation Analysis using the Texas Cold Neutron Source, Ph.D. Dissertation, The University of Texas at Austin, 1995.
11. Y. GYUN JO, Development of a Thermal Neutron Imaging Facility for Real Time Neutron Radiography and Computed Tomography, Ph.D. Dissertation, The University of Texas at Austin, 1998.
12. D. J. DORSEY, W. S. CHARLTON, Trans. Am. Nucl. Soc., 88 (2003) 666.
13. G. L. MOLNÁR, ZS. RÉVAY, T. BELGYA, Nucl. Instr. Meth. Phys. Res., A489 (2002) 140.
14. D. J. DORSEY, W. S. CHARLTON, R. HEBNER, Trans. Am. Nucl. Soc., 86 (2002) 389.
15. H. D. CHOI, R. B. FIRESTONE, R. M. LINDSTROM, G. L. MOLNÁR, A. REDDY, V. H. TAN, C. M. ZHOU, R. PAVIOTTI-CORCUERA, A. TRKOV, Trans. of the International Conf. on Nuclear Data for Science and Technology, Tsukuba, Japan, 2002.
16. D. L. SMITH, LSMOD/GLSMOD: A Least-Squares Computational 'Tool Kit', ANL/NDM-128, Argonne National Laboratory, 1993.
17. R. C. REEDY, S. C. FRANKLE, Atomic Data and Nuclear Data Tables, 80 (2002) 1.